

SCIENTIFIC REPORTS



OPEN

Investigation of the Hydrolysis of Perovskite Organometallic Halide $\text{CH}_3\text{NH}_3\text{PbI}_3$ in Humidity Environment

Received: 10 December 2015

Accepted: 02 February 2016

Published: 29 February 2016

Jiangtao Zhao¹, Bing Cai², Zhenlin Luo¹, Yongqi Dong¹, Yi Zhang¹, Han Xu¹, Bin Hong¹, Yuanjun Yang¹, Liangbin Li¹, Wenhua Zhang² & Chen Gao¹

Instability of emerging perovskite organometallic halide in humidity environment is the biggest obstacle for its potential applications in solar energy harvest and electroluminescent display. Understanding the detailed decay mechanism of these materials in moisture is a critical step towards the final appropriate solutions. As a model study presented in this work, *in situ* synchrotron radiation x-ray diffraction was combined with microscopy and gravimetric analysis to study the degradation process of $\text{CH}_3\text{NH}_3\text{PbI}_3$ in moisture, and the results reveal that: 1) intermediate monohydrated $\text{CH}_3\text{NH}_3\text{PbI}_3 \cdot \text{H}_2\text{O}$ is detected in the degradation process of $\text{CH}_3\text{NH}_3\text{PbI}_3$ and the final decomposition products are PbI_2 and aqueous $\text{CH}_3\text{NH}_3\text{I}$; 2) the aqueous $\text{CH}_3\text{NH}_3\text{I}$ could hardly further decompose into volatile CH_3NH_2 , HI or I_2 ; 3) the moisture disintegrate $\text{CH}_3\text{NH}_3\text{PbI}_3$ and then alter the distribution of the decomposition products, which leads to an incompletely-reversible reaction of $\text{CH}_3\text{NH}_3\text{PbI}_3$ hydrolysis and degrades the photoelectric properties. These findings further elucidate the picture of hydrolysis process of perovskite organometallic halide in humidity environment.

Nowadays, solar cells which use perovskite organometallic halide as light absorption layer have aroused a vast concern all over the world, due to the merits of high efficiency, low-cost and simple synthesis process of the perovskite materials^{1–12}. In 2009, power conversion efficiency (PCE) of 3.81% was firstly demonstrated in perovskite solar cell with spin-coated $\text{CH}_3\text{NH}_3\text{PbI}_3$ on FTO¹. Six years later, PCE as high as ~20% has been acquired through continuous efforts in controlling the formation of the perovskite layer and choosing appropriate material for other layers^{2–7}. The quickly enhanced PCE seems signal a new era of perovskite solar cells.

Unfortunately, the instability of organometallic halide perovskite in humidity environment is a tough problem, which hinders its practical application in solar cells and electroluminescent display. Therefore, it is urgent to make clear the decay mechanism of this easily air-slaked material, which is fundamentally meaningful and is also a critical step for pursuing more appropriate solutions. As a model system of perovskite organometallic halide, $\text{CH}_3\text{NH}_3\text{PbI}_3$ has been intensively studied recently, including the instability problem in moisture^{13–20}. For instance, in 2014, Niu and Frost *et al* proposed a set of degradation equations¹⁶ and a possible decomposition pathway¹⁷, respectively. Thereafter, more experimental evidences were reported by Yang¹⁸, Christians¹⁹ and Leguy²⁰ *et al*. Yang and co-workers utilized *in situ* grazing incidence X-ray diffraction to monitor the phase evolution of $\text{CH}_3\text{NH}_3\text{PbI}_3$ in water vapor, where an intermediate phase was found and supposed to be $(\text{CH}_3\text{NH}_3)_4\text{PbI}_6 \cdot 2\text{H}_2\text{O}$ ¹⁸. This intermediate phase was also discovered by Christians *et al*¹⁹. Moreover, Leguy *et al* reported a more systematic work performed with time-resolved XRD and ellipsometry, in which two different hydrated crystalline phases of $\text{CH}_3\text{NH}_3\text{PbI}_3$, i.e., $\text{CH}_3\text{NH}_3\text{PbI}_3 \cdot \text{H}_2\text{O}$ and $(\text{CH}_3\text{NH}_3)_4\text{PbI}_6 \cdot 2\text{H}_2\text{O}$ were detected and a suite of convincing degradation equations were provided²⁰. However, despite all these, more detailed questions should be answered, like ‘what are the real final decomposition products?’ and ‘what is the function of moisture in the degradation process?’

¹National Synchrotron Radiation Laboratory and CAS Key Laboratory of Materials for Energy Conversion, University of Science and Technology of China, Hefei, Anhui, 230026, China. ²State Key Laboratory of Catalysis, Dalian Institute of Chemical Physics, Chinese Academy of Sciences, Dalian National Laboratory for Clean Energy, Dalian 116023, China. Correspondence and requests for materials should be addressed to Z.L. (email: zlluo@ustc.edu.cn) or C.G. (email: cgao@ustc.edu.cn)

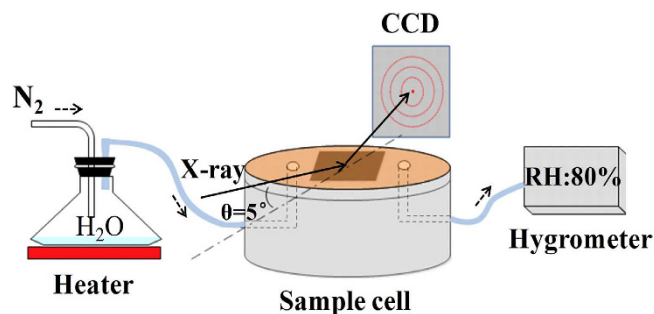


Figure 1. Schematic diagram of the RH control device and the diffraction geometry in the *in-situ* XRD experiment.

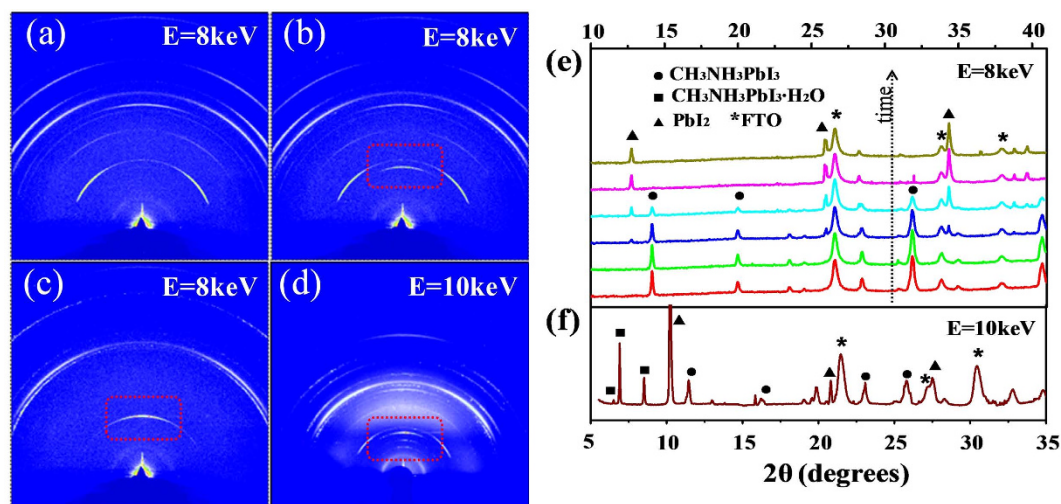


Figure 2. *In situ* XRD patterns. (a–d) Typical diffraction patterns of spin-coated $\text{CH}_3\text{NH}_3\text{PbI}_3/\text{FTO}$ in degradation process and (e–f) the corresponding integral curves obtained by using Fit2D program.

To address these issues, here, we carefully studied the degradation process of typical perovskite organometallic halide $\text{CH}_3\text{NH}_3\text{PbI}_3$ in moisture. Using *in-situ* synchrotron XRD experiment, four distinct states have been revealed and in which monohydrated $\text{CH}_3\text{NH}_3\text{PbI}_3 \cdot \text{H}_2\text{O}$ and one decomposition product PbI_2 are found. Another decomposition product, $\text{CH}_3\text{NH}_3\text{I}$, is confirmed through a solid-liquid separation experiment and it was demonstrated to be difficult for aqueous $\text{CH}_3\text{NH}_3\text{I}$ to transform to volatile matter through a gravimetric analysis. The microscopy analysis reveals that the reaction of $\text{CH}_3\text{NH}_3\text{PbI}_3$ with water vapor is not a completely reversible one, because the moisture alters the distribution of decomposition products and thus partially separates PbI_2 and $\text{CH}_3\text{NH}_3\text{I}$.

Results and Discussion

***In situ* synchrotron radiation XRD experiment.** Figure 1 is the schematic of the experiment setup, in which $\text{CH}_3\text{NH}_3\text{PbI}_3/\text{FTO}$ film was placed in a homemade sample cell at the diffractometer center. The relative humidity (RH) in the cell was controlled by tuning the flow rate of nitrogen gas and the temperature of the heater. The RH value was real-time monitored by a commercial hygrometer and which was regulated to about 80% during the whole experiment. To confine the moisture, the cell was sealed with kapton film which will not block the incident and diffractive x-ray beam passing through.

Figure 2 shows the typical diffraction patterns selected from the large set of data collected during the *in situ* synchrotron radiation XRD experiment, which indicates the degradation process of spin-coated $\text{CH}_3\text{NH}_3\text{PbI}_3/\text{FTO}$ in moisture.

Figure 2a–c are three typical patterns taken during one test (X-ray photon energy $E = 8\text{keV}$) with a time sequence of $a \rightarrow b \rightarrow c$, and the corresponding integrated curves are presented in Fig. 2e among those belong to the time-serial data set. Figure 2a is the diffraction pattern of the as-grown $\text{CH}_3\text{NH}_3\text{PbI}_3/\text{FTO}$ without water vapor around the sample, which reveals that the film is polycrystalline with preferred orientation along the normal direction. As shown in Fig. 2b, with the time increasing in a relative humidity of $80 \pm 5\%$, the diffraction peaks of perovskite $\text{CH}_3\text{NH}_3\text{PbI}_3$ gradually decrease due to degradation and the reflections belonging to PbI_2 (PDF#07-0235) become more and more intense. Figure 2c shows that the final decomposition product is composed mainly by PbI_2 . However, according to the law of conservation of elements, at least another decomposition product should be there. Since no obvious peaks from other phases appear in this pattern, that product is believed

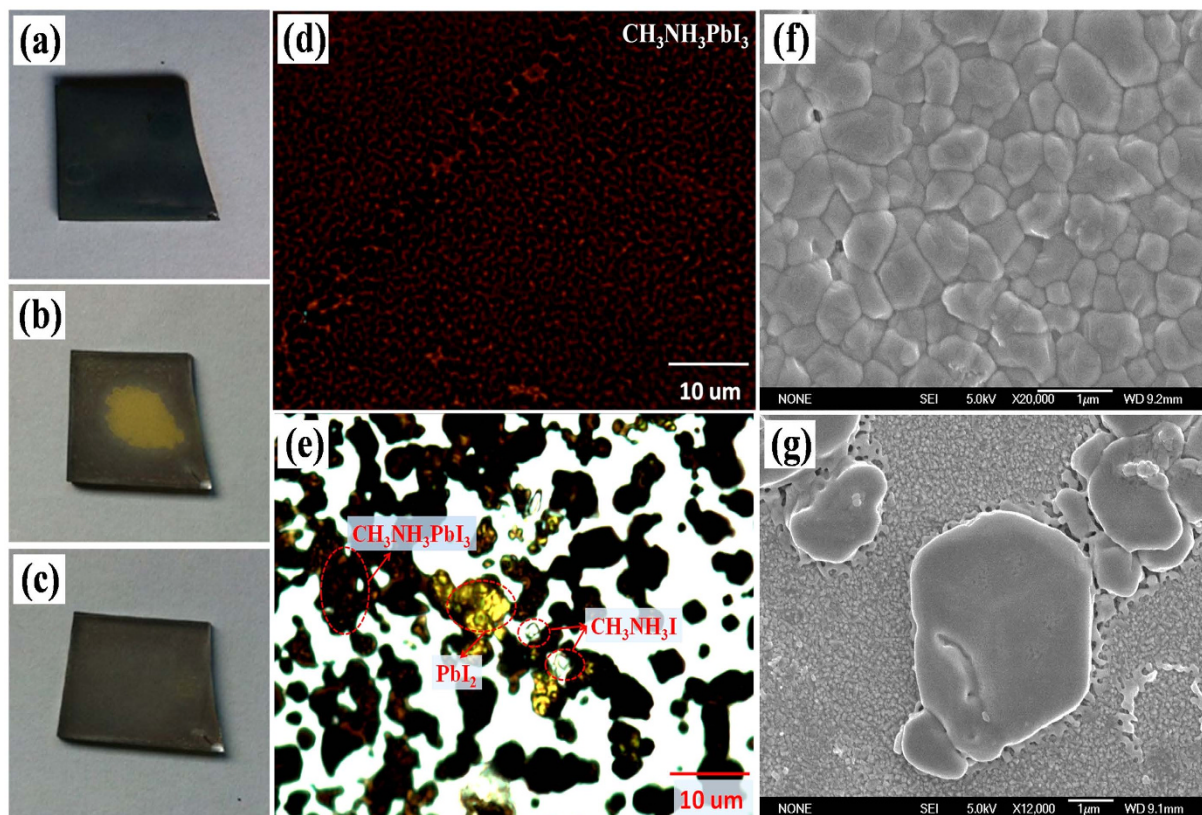


Figure 3. Microscopy images of $\text{CH}_3\text{NH}_3\text{PbI}_3/\text{FTO}$ film before and after decaying. (a) Photographs of the as-grown $\text{CH}_3\text{NH}_3\text{PbI}_3/\text{FTO}$ film and (b,c) the decayed $\text{CH}_3\text{NH}_3\text{PbI}_3$ films after taken out from the moisture. (d) Optical micrographs of the as-grown $\text{CH}_3\text{NH}_3\text{PbI}_3/\text{FTO}$ film and (e) the decayed $\text{CH}_3\text{NH}_3\text{PbI}_3$ film. (f) SEM images of the as-grown $\text{CH}_3\text{NH}_3\text{PbI}_3/\text{FTO}$ film and (g) the decayed $\text{CH}_3\text{NH}_3\text{PbI}_3$ film.

to be volatilized or dissolved in water. As described in detail in the following part, the product is proved to be aqueous $\text{CH}_3\text{NH}_3\text{I}$.

When we repeated the *in situ* XRD measurements, sometimes, we could fortunately detect a metastable phase during the degradation process. One of such patterns is presented in Fig. 2d and the integral curve is plotted in Fig. 2f. The peaks at 6.5° , 6.9° and 8.5° are ascribed to the (001), (110) and ($\bar{1}01$) reflections of the metastable monoclinic $\text{CH}_3\text{NH}_3\text{PbI}_3 \cdot \text{H}_2\text{O}$ ²⁰. Please note that such intermediate phases were not obvious every time during our XRD experiments, because it is difficult to catch these time- and space-limited phases without enough diffraction intensity by using x-ray beam with sub-millimeter size. Of course, it is more possible to detect such hydrates if people delay the degradation process by decreasing the relative humidity around the sample.

Microscopy Analysis. During the *in situ* XRD experiment, the as-grown brown black $\text{CH}_3\text{NH}_3\text{PbI}_3/\text{FTO}$ film (Fig. 3a) gradually becomes yellow (Fig. 3b) in the humidity environment. But, it is interesting that the surface of the film slowly turns yellow to light black (Fig. 3c) after we take the film out of the humidity condition, which seems should be attributed to the water evaporating from the sample.

This phenomenon combined with XRD results (data not show here) indicates the reaction between $\text{CH}_3\text{NH}_3\text{PbI}_3$ and water vapor is not fully reversible. We guess the underlying cause is that the water vapor not only decompose $\text{CH}_3\text{NH}_3\text{PbI}_3$ into PbI_2 and aqueous $\text{CH}_3\text{NH}_3\text{I}$, but also separates these products to some degree. To demonstrate this hypothesis, optic microscopy and scanning electron microscopy (SEM) were utilized to investigate the film morphology before and after the degradation.

Figure 3d is a typical optical micrograph of the as-grown spin-coated $\text{CH}_3\text{NH}_3\text{PbI}_3/\text{FTO}$ film. The uniform brown black color indicates the film is homogeneous without obvious second phase. Similar distribution state is also revealed from the corresponding SEM image (Fig. 3f). For the film after the degradation, three types of grain with different color could be easily recognized from the optical micrograph Fig. 3e. The yellow particles are PbI_2 , bright transparent grains should be $\text{CH}_3\text{NH}_3\text{I}$, and the brown black ones are the revived $\text{CH}_3\text{NH}_3\text{PbI}_3$. In addition, the distribution of these color grains were found in an obvious isolated and disorder manner in comparison with the initial $\text{CH}_3\text{NH}_3\text{PbI}_3$ film. The SEM image in Fig. 3g also clearly illustrates the rough morphology of the decayed $\text{CH}_3\text{NH}_3\text{PbI}_3$ film. The above microscopy analysis proves that the moisture indeed alters the distribution of decomposition products and thus makes the reverse reaction between $\text{CH}_3\text{NH}_3\text{PbI}_3$ and water insufficient.

Till now, the degradation process and decay mechanism may be expressed as follows:

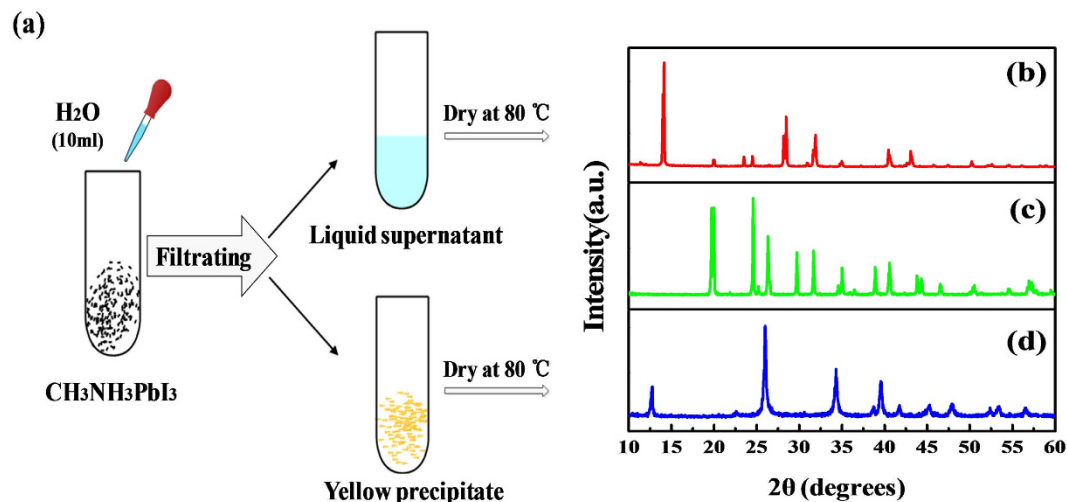
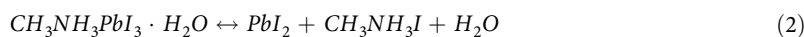
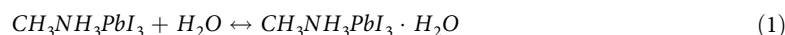


Figure 4. (a) Schematic diagram of solid-liquid separation experiment; XRD patterns of (b) $\text{CH}_3\text{NH}_3\text{PbI}_3$ powder, (c) the resulting powder separated out from the liquid supernatant and (d) dried yellow precipitate.



Solid-Liquid Separation Methods and Gravimetric Analysis. As shown in the microscope images, the separation of PbI_2 and $\text{CH}_3\text{NH}_3\text{I}$ in real space is the key step towards the irreversible reaction between $\text{CH}_3\text{NH}_3\text{PbI}_3$ and water. The cause of this separation is thought to be the different solubility of PbI_2 and $\text{CH}_3\text{NH}_3\text{I}$ in water, which is verified by the following solid-liquid separation experiment.

Here, $\text{CH}_3\text{NH}_3\text{PbI}_3$ powder is used as the research object to make things simple and clear. The steps of the experiment are schematically shown in Fig. 4a. First, $\text{CH}_3\text{NH}_3\text{PbI}_3$ powder (XRD pattern presented in Fig. 4b) was put in distilled water, and the black powder was found turned into yellow precipitate at once. Then, the liquid supernatant and the yellow precipitate were separated by centrifuging and filtrating. Both the liquid supernatant and yellow precipitate were dried at 80°C in dark and the resulting powders were characterized by XRD (Fig. 4c,d), respectively.

From the XRD patterns, it is found that the soluble product of $\text{CH}_3\text{NH}_3\text{PbI}_3$ hydrolysis is $\text{CH}_3\text{NH}_3\text{I}$ (PDF#10-0737) and the yellow precipitate is PbI_2 (PDF#07-0235). The difference in solubility of these two products is the major reason for separation.

Back to the aforementioned another question, i.e. ‘what are the real final decomposition products of $\text{CH}_3\text{NH}_3\text{PbI}_3$ hydrolysis’, previous studies mostly claim that the final rest product is PbI_2 while the aqueous $\text{CH}_3\text{NH}_3\text{I}$ will volatilize as CH_3NH_2 , HI or I_2 in the condition of moisture and sunlight. Detailed information can be found in ref.16,17,21. Noted that $\text{CH}_3\text{NH}_3\text{PbI}_3/\text{TiO}_2/\text{FTO}$ hetero-structure was used in these studies, it could not exclude the interfacial effect²¹ in $\text{CH}_3\text{NH}_3\text{PbI}_3/\text{TiO}_2$ since TiO_2 is well-known photocatalytic material²². Therefore, another question emerged naturally is what the hydrolysis products of stand-alone $\text{CH}_3\text{NH}_3\text{PbI}_3$. Here, a high-precision gravimetric analysis has been carried out to investigate whether the aqueous $\text{CH}_3\text{NH}_3\text{I}$ will further volatilize for $\text{CH}_3\text{NH}_3\text{PbI}_3$ powders, and the results are listed in Fig. 5. First, two sets of 0.621g $\text{CH}_3\text{NH}_3\text{PbI}_3$ powder and two sets of 0.320g $\text{CH}_3\text{NH}_3\text{I}$ powder were put in test tubes separately, and then 5 ml distilled water was injected in each test tube. Next, one set of watered $\text{CH}_3\text{NH}_3\text{PbI}_3$ and one set of aqueous $\text{CH}_3\text{NH}_3\text{I}$ were directly dried in dark, i.e. in the drying oven at 80°C for a week, while the rest were dried in sunlight for the same time. Finally, all the dried powders were weighted using electronic balance with a precision of 0.01 mg.

The 1st row in Fig. 5 reveals the color and weight change of $\text{CH}_3\text{NH}_3\text{PbI}_3$ powder in this experiment. Notice that the $\text{CH}_3\text{NH}_3\text{PbI}_3$ decayed in water changes back to black again either dried in dark or in sunlight, which confirm that the reaction between $\text{CH}_3\text{NH}_3\text{PbI}_3$ and water is almost reversible if the decomposition products are not separated. As shown by the weight values listed in the figure, the $\text{CH}_3\text{NH}_3\text{PbI}_3$ powder almost does not lose any weight either dried in dark or in sunlight, which indicates that no obvious volatile matter release during $\text{CH}_3\text{NH}_3\text{PbI}_3$ hydrolysis, i.e. it is hard for $\text{CH}_3\text{NH}_3\text{I}$ to further separate. The conclusion was also verified by the control experiment performed on $\text{CH}_3\text{NH}_3\text{I}$ powder, in which the results listed in the 2nd row show that the $\text{CH}_3\text{NH}_3\text{I}$ powder weight almost does not reduce in any cases. In the above measurements, no reflections from other phases were detected by XRD before and after gravimetric analysis (data not shown here). Please note that, the results and conclusion presented here are much different from that found in $\text{CH}_3\text{NH}_3\text{PbI}_3/\text{TiO}_2/\text{FTO}$ hetero-structure, indicating TiO_2 could influence the degradation process of $\text{CH}_3\text{NH}_3\text{PbI}_3$.

Now, it could be said that the above decay equations (1 and 2) are the major reaction for stand-alone $\text{CH}_3\text{NH}_3\text{PbI}_3$, and the electric transport layer (ETL) in perovskite solar cells may affect the stability of perovskite

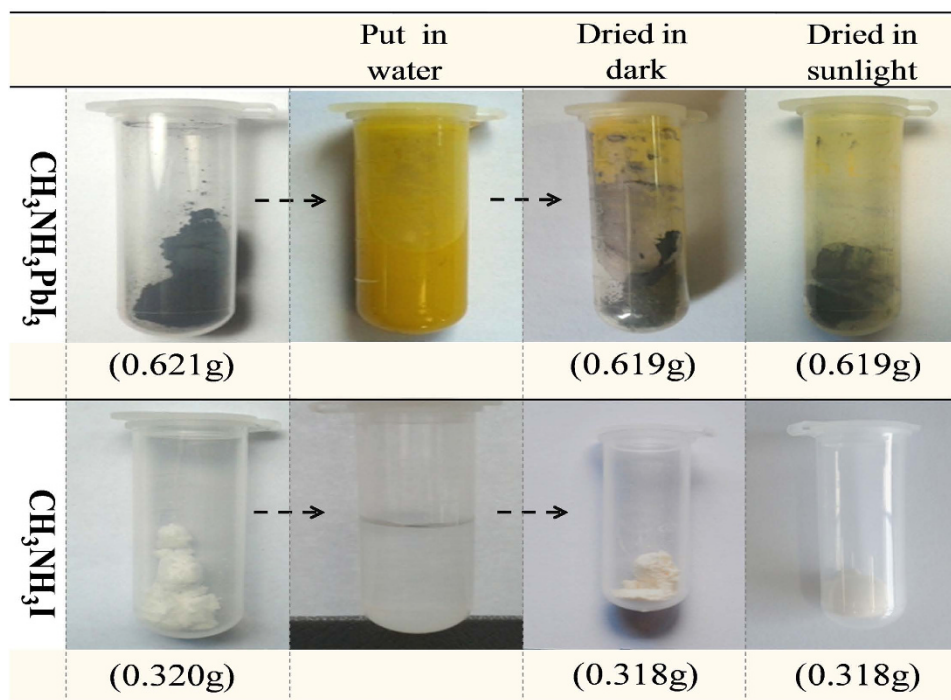


Figure 5. Color and weight change of $\text{CH}_3\text{NH}_3\text{PbI}_3$ (1st row) and $\text{CH}_3\text{NH}_3\text{I}$ (2nd row) powder when dried in dark or sunlight.

organometallic halides^{23–26}. Our findings in this paper further elucidate the picture of hydrolysis process of this perovskite material in humidity environment.

Conclusion

Based on *in situ* synchrotron radiation XRD, a reasonable decomposition pathway for $\text{CH}_3\text{NH}_3\text{PbI}_3$ materials in moisture is proposed and the intermediate monohydrated $\text{CH}_3\text{NH}_3\text{PbI}_3 \cdot \text{H}_2\text{O}$ is detected during the degradation process. Moreover, the function of moisture was further investigated via microscopy and gravimetric analysis. The results show that moisture not only decompose $\text{CH}_3\text{NH}_3\text{PbI}_3$ into PbI_2 and aqueous $\text{CH}_3\text{NH}_3\text{I}$ but also altered their distribution, which result in poor connection between PbI_2 and $\text{CH}_3\text{NH}_3\text{I}$ and thus leads to an incompletely-reversible reaction of $\text{CH}_3\text{NH}_3\text{PbI}_3$ hydrolysis. Furthermore, it is confirmed that the final products of $\text{CH}_3\text{NH}_3\text{PbI}_3$ hydrolysis are just PbI_2 and aqueous $\text{CH}_3\text{NH}_3\text{I}$, and $\text{CH}_3\text{NH}_3\text{I}$ will hardly further decompose into volatile CH_3NH_2 , HI or I_2 for $\text{CH}_3\text{NH}_3\text{PbI}_3$ itself. The degradation process and decay mechanism of perovskite $\text{CH}_3\text{NH}_3\text{PbI}_3$ in moisture becomes clearer with this work, which is believed to be helpful to understand the instability problem in moisture of various perovskite organometallic halides and figure out the possible solutions according to their applications.

Methods

To prepare the $\text{CH}_3\text{NH}_3\text{PbI}_3$ specimens, equimolar $\text{CH}_3\text{NH}_3\text{I}$ and PbI_2 (98%, Sinopharm) were mixed in γ -butyrolactone (97%, Sinopharm) at 60 °C overnight whilst being stirred. Then, the aqueous precursor was deposited on FTO glass by spin-coating at 2000 rpm for 40s. Finally, the specimens were annealed at 100 °C for 15 min on a preheated hot plate, and the obtained $\text{CH}_3\text{NH}_3\text{PbI}_3/\text{FTO}$ films were brown black²⁷.

In situ synchrotron radiation XRD was performed at the BL14B station of Shanghai Synchrotron Radiation Facility (SSRF), and the experimental setup is schematically shown in Fig. 1. The diffractive patterns were recorded by a two-dimension x-ray detector (charge coupled device, CCD) with 3072×3072 pixels. To monitor the reaction at real-time, the diffraction patterns were continuously recorded with 10 seconds per frame and 1 second between adjacent frames.

To investigate the $\text{CH}_3\text{NH}_3\text{PbI}_3$ film morphology before/after the reaction, microscopy analysis was performed by using optical microscope (OLYMPUS, BX51) and scanning electron microscope (SEM, JSM-6700F).

References

- Kokima, A., Teshima, K., Shirai, Y. & Miyasaka. Organometal halide perovskites as visible-light sensitizers for photovoltaic cells. *J. Am. Chem. Soc.* **131**, 6050–6051 (2009).
- Im, J. H., Lee, C. R., Lee, J. W., Park, S. W. & Park, N. G. 6.5% efficient perovskite quantum-dot-sensitized solar cell. *Nanoscale* **3**, 4088–4093 (2011).
- Kim, H. S. *et al.* Lead iodide perovskite sensitized all-solid-state submicron thin film mesoscopic solar cell with efficiency exceeding 9%. *Sci. Rep.* **2**, 591, doi: 10.1038/srep00591 (2012).
- Liu, M. Z., Johnston, M. B. & Snaith, H. J. Efficient planar heterojunction perovskite solar cells by vapour deposition. *Nature* **501**, 395–398 (2013).

5. Jeon, N. J. *et al.* Solvent engineering for high-performance inorganic–organic hybrid perovskite solar cells. *Nature materials* **13**, 897–903 (2014).
6. Zhou, H. P. *et al.* Interface engineering of highly efficient perovskite solar cells. *Science* **345**, 542–546 (2014).
7. Best Research cells efficiencies. http://www.nrel.gov/ncpv/images/efficiency_chart.jpg, Date of access: 30/12/2014.
8. Saidaminov, M. I. *et al.* High-quality bulk Hybrid perovskite single crystals within minutes by inverse temperature crystallization. *Nat. Commun.* **6**, 7586, doi: 10.1038/ncomms8586 (2015).
9. Dong, Q. F. *et al.* Electron-hole diffusion lengths > 175 μm in solution-grown $\text{CH}_3\text{NH}_3\text{PbI}_3$ single crystals. *Science* **347**, 967–970 (2015).
10. Dou, L. T. *et al.* Atomically thin two-dimensional organic–inorganic hybrid perovskites. *Science* **349**, 1518–1521 (2015).
11. Liu, Y. C. *et al.* Two-Inch-Sized perovskite $\text{CH}_3\text{NH}_3\text{PbX}_3$ (X = Cl, Br, I) crystals: growth and characterization. *Adv. Mater.* **27**, 5176–5183 (2015).
12. Wong, A. B. *et al.* Growth and anion exchange conversion of $\text{CH}_3\text{NH}_3\text{PbX}_3$ nanorod arrays for light-emitting diodes. *Nano Lett.* **15**, 5519–5524 (2015).
13. GRÄTZEL, M. & Park, N. G. Organometal halide perovskite photovoltaics: A diamond in the rough. *Nano* **09**, 1440002, doi: 10.1142/S1793292014400025 (2014).
14. Niu, G. D., Guo, X. D. & Wang L. D. Review of recent progress in chemical stability of perovskite solar cells. *J. Mater. Chem. A* **3**, 8970–8980 (2015).
15. Dong, X. *et al.* Improvement of the humidity stability of organic–inorganic perovskite solar cells using ultrathin Al_2O_3 layers prepared by atomic layer deposition. *J. Mater. Chem. A* **3**, 5360–5367 (2015).
16. Niu, G. D. *et al.* Study on the stability of $\text{CH}_3\text{NH}_3\text{PbI}_3$ films and the effect of post-modification by aluminum oxide in all-solid-state hybrid solar cells. *J. Mater. Chem. A* **2**, 705–710 (2014).
17. Frost, J. M. *et al.* Atomistic origins of high-performance in hybrid halide perovskite solar cells. *Nano Lett.* **14**, 2584–2590 (2014).
18. Yang, J. L., Siempelkamp, B. D., Liu, D. Y. & Kelly, T. L. Investigation of $\text{CH}_3\text{NH}_3\text{PbI}_3$ degradation rates and mechanisms in controlled humidity environments using *in situ* techniques. *ACS Nano* **9**, 1955–1963 (2015).
19. Christians, J. A., Miranda Herrera, P. A. & Kamat, P. V. Transformation of The Excited State and Photovoltaic Efficiency of $\text{CH}_3\text{NH}_3\text{PbI}_3$ Perovskite upon Controlled Exposure to Humidified Air. *J. Am. Chem. Soc.* **137**, 1530–1538 (2015).
20. Leguy, A. M. A. *et al.* Reversible Hydration of $\text{CH}_3\text{NH}_3\text{PbI}_3$ in films, Single Crystals and Solar Cells. *Chem. Mater.* **27**, 3397–3407 (2015).
21. Ito, S., Tanaka, S., Manabe, K. & Nishino, H. Effects of surface blocking layer of Sb_2S_3 on nanocrystalline TiO_2 for $\text{CH}_3\text{NH}_3\text{PbI}_3$ perovskite solar cells. *J. Phys. Chem. C* **118**, 16995–17000 (2014).
22. Chen, X. B. & Mao, S. S. Titanium dioxide nanomaterials: synthesis, properties, modifications and applications. *Chem. Rev.* **107**, 2891–2959 (2007).
23. Mali, S. S., Shim, C. S. & Hong, C. K. Highly porous zinc stannate (Zn_2SnO_4) nanofibers scaffold photoelectrodes for efficient methyl ammonium halide perovskite solar cells. *Sci. Rep.* **5**, 11424, doi: 10.1038/srep11424 (2015).
24. Bera, A. *et al.* Fast crystallization and improved stability of perovskite solar cells with Zn_2SnO_4 electron transporting layer: interface matters. *ACS Appl. Mater. Interfaces* **7**, 28404–28411 (2015).
25. Mali, S. S. *et al.* Ultrathin atomic layer deposited TiO_2 for surface passivation of hydrothermally grown 1D TiO_2 nanorod arrays for efficient solid-state perovskite solar cells. *Chem. Mater.* **17**, 1541–1551 (2015).
26. You, J. B. *et al.* Improved air stability of perovskite solar cells via solution-processed metal oxide transport layers. *Nature Nanotech.* **11**, 75–81 (2016).
27. Cai, B., Xing, Y. D., Yang, Z., Zhang, W. H. & Qiu, J. S. High performance hybrid solar cells sensitized by organolead halide perovskites. *Energy Environ. Sci.* **6**, 1480–1485 (2013).

Acknowledgements

The authors thank the staff at beamline BL14B of SSRF for their support. This work was financially supported by the National Natural Science Foundation of China (11374010 and 11434009) and the Fundamental Research Funds for the Central Universities.

Author Contributions

J.Z. and Z.L. designed the experiment. B.C. and W.Z. carried out synthesis of materials. J.Z., Z.L., Y.D., H.X. and C.G. performed the *in situ* XRD experiment and data analysis. Microscopy analysis and the rest experiment were performed by B.H., Y.Z., Y.Y. and L.L. The paper was written by J.Z. and Z.L. All authors reviewed and commented on the manuscript.

Additional Information

Competing financial interests: The authors declare no competing financial interests.

How to cite this article: Zhao, J. *et al.* Investigation of the Hydrolysis of Perovskite Organometallic Halide $\text{CH}_3\text{NH}_3\text{PbI}_3$ in Humidity Environment. *Sci. Rep.* **6**, 21976; doi: 10.1038/srep21976 (2016).



This work is licensed under a Creative Commons Attribution 4.0 International License. The images or other third party material in this article are included in the article's Creative Commons license, unless indicated otherwise in the credit line; if the material is not included under the Creative Commons license, users will need to obtain permission from the license holder to reproduce the material. To view a copy of this license, visit <http://creativecommons.org/licenses/by/4.0/>